Journal of Engineering Research and Applied Science
Available at www.journaleras.com
Volume 12 (2), December 2023, pp 2382-2394
ISSN 2147-3471 © 2023

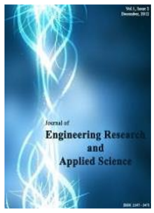

Geochemistry and petrogenesis of the Late Cretaceous Büyükdüz Gabbro (Trabzon, NE Turkey)

Abdullah Kaygusuz

Gümüşhane University, Geological Engineering, Gümüşhane, Turkey

Accepted 25 November 2023

Abstract

Late Cretaceous I-type plutons are widespread in the Eastern Pontides orogenic belt (EPOB), NE Turkey. Although the majority of the plutons in the EPOB are diorite to granite in composition, very few contains gabbro composition. In this study, we report petrographic and whole-rock geochemical compositions of the Büyükdüz Gabbro. The rocks of the Büyükdüz Gabbro has a uniform composition and is gabbro in composition. The rocks mainly consist of plagioclase, pyroxene, hornblende and Fe-Ti oxide minerals. They are I-type, low to medium-K calc-alkaline, and metaluminous characters, and have low SiO_2 content (51-53 wt.%) and moderate Mg number (Mg# = 54-59). Decreasing CaO, MgO, Fe_2O_3, TiO_2, P_2O_5, Ni, Y and Sr with increasing SiO_2 contents are consistent with fractional crystallization of plagioclase, clinopyroxene and hornblende. The studied rocks are enriched in large-ion lithophile elements (LILEs) and light rare-earth elements (LREEs). Chondrite normalized REE patterns of the samples are concave shaped (La_N/Yb_N = 3.8-8.8) and display negative Eu (Eu_N/Eu^* = 0.77-0.84) anomalies. All these data with regional geology indicates that the parental magma of the studied rocks derived from an enriched lithospheric mantle source in an arc setting.

Keywords: *Büyükdüz Gabbro, Eastern Pontides (NE Turkey), Late Cretaceous, Geochemistry, Petrogenesis*

1. Introduction

The EPOB in NE Turkey, located in the Alpine-Himalayan orogenic belt, is one of the well-preserved continental magmatic arcs [1,2] where plutonic and volcanic rocks are widely observed [3–9]. The plutonic rocks varying ages from Early Carboniferous to Eocene are located in this region. These plutons were emplaced in four different time periods: Early Carboniferous, Middle-Late Jurassic, Late Cretaceous and Eocene. The compositions of these plutons vary from gabbro to granite, although gabbro compositions are not common.

Numerous geochemical and petrological studies have been conducted on Late Cretaceous plutons of the EPOB [10,11]. However, studies on the Büyükdüz Gabbro are scarce [12]. In this study, we report petrographic and whole-rock geochemical compositions of the Büyükdüz Gabbro to determine their magma parental sources.

2. Material and Method

The whole-rock geochemical analysis of the rock samples, which were compiled from the study area, were carried out in the ACME Analytical Chemical Laboratory (Vancouver, Canada). Major and trace elements were analyzed by ICP-AES method and rare earth elements (REEs) were analyzed by ICP-MS method. Details of analysis technique are given in [11].

3. Regional and local geology

The Eastern Pontides is commonly subdivided into southern and northern zones [2,13]. The study area is located in the northern zone of the EPOB (Fig. 1).

The pre-Late Cretaceous units in the EPOB consist mainly of Early Carboniferous metamorphic rocks [14], Late to Early Carboniferous plutonic rocks [15–22], Early and Middle Jurassic volcano-sedimentary rocks [23,24], Mid to Late Jurassic plutonic rocks [25–28] and Late Jurassic to Early Cretaceous carbonates [29]. Late Cretaceous units, including the studied Büyükdüz Gabbro, consist of plutonic, volcanic and sedimentary rocks [30–37]. Cenozoic units consist of plutonic-volcanic (adakitic and non-adakitic) and sedimentary rocks [38,39,48,49,40–47]. Quaternary alluvium forms the youngest units in the region.

Corresponding author: abdullah.kaygusuz@gmail.com

The oldest units in the studied area comprise Liassic aged Hamurkesen Formation consisting of mainly basalt, andesite and pyroclastic rocks. Late Cretaceous aged Çatak Formation consisting of andesite, basalt and pyroclastic rocks lie unconformably on these units. All these units were cut by Late Cretaceous aged Camiboğazı Pluton and Büyükdüz Gabbro.

Büyükdüz gabbro is approximately ellipse-shaped and the long axis extends in the northwest-southeast direction (Figure 1). It is dark colored in the field and is rich in mafic minerals.

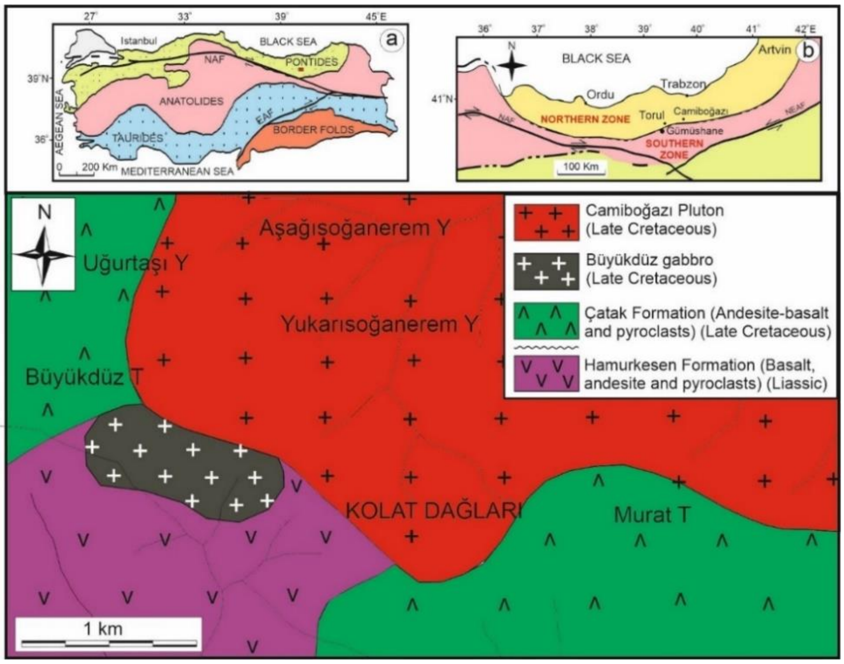

Figure 1. Geological map of the study area (modified after [11]

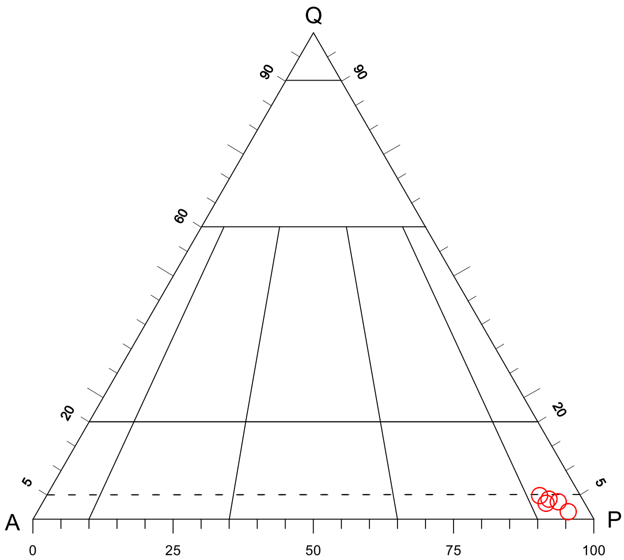

Figure 2. Classification based on modal compositions of the Büyükdüz gabbroic rocks [50].

4. Results

4.1. Petrography

The Büyükdüz gabbroic rocks are gabbro in compositions in the modal QAP diagram (Figure 2) [50].

The studied gabbroic rocks are generally holocrystalline, medium to coarse grained. All samples from the studied rocks consist of equigranular plagioclase (modal 68 to 71%), clinopyroxene (6 to 9%) and hornblende (10 to 12%) as major mineral phases. Apatite, zircon and Fe-Ti oxides form accessory minerals. Secondary phases comprise sericite, calcite, chlorite and clay minerals (Table 1). Plagioclases form euhedral and subhedral lath-shaped phenocrysts. Clinopyroxenes are found as subhedral to anhedral, weakly-zoned grains and also in aggregates. Hornblends are in the form of euhedral prismatic crystals and contain small apatite and opaque minerals as inclusions. They have well developed cleavages. Subhedral to anhedral apatites are relatively abundant accessory minerals. Zircons are seen as small euhedral prismatic crystals. Opaque minerals are found as subhedral and euhedral in both small and large crystals.

4.2. Whole-rock Geochemistry

4.2.1. Major and trace elements

Considering the results of the geochemical analysis, the SiO_2 values of the rock samples from the Büyükdüz Gabbro vary between 51 and 53 wt.%, while their MgO content varies between 4.9 and 6.2 wt.% (Table 1). The K_2O/Na_2O ratios are less than 1 and are between 0.2 and 0.5. A/CNK values are between 0.8 and 0.9, and the magnesium numbers [Mg#=100*(MgO/MgO+$Fe_2O_3^T$)] are between 54 and 59 (Table 1).

Table 1. The whole-rock major, trace and REE element analysis of the studied samples

	Min	Max	Avg			Min	Max	Avg
SiO_2	50.96	52.94	51.68		La	9.20	21.90	15.58
TiO_2	0.42	0.54	0.49		Ce	19.50	50.60	31.28
Al_2O_3	16.93	17.96	17.40		Pr	2.28	5.75	3.82
$Fe_2O_3^T$	8.42	9.45	9.01		Nd	10.00	23.80	16.68
MnO	0.16	0.19	0.18		Sm	2.35	4.20	3.42
MgO	4.86	6.17	5.41		Eu	0.67	0.99	0.86
CaO	7.53	9.71	8.81		Gd	2.51	3.28	2.96
Na_2O	2.12	2.46	2.29		Tb	0.42	0.55	0.49
K_2O	0.34	1.34	0.94		Dy	2.66	2.92	2.77
P_2O_5	0.05	0.09	0.07		Ho	0.55	0.67	0.60
LOI	3.40	3.70	3.52		Er	1.52	1.75	1.65
Total	99.73	99.85	99.78		Tm	0.21	0.27	0.24
Ni	9.20	15.80	11.74		Yb	1.63	1.84	1.72
V	149.00	213.00	190.40		Lu	0.24	0.27	0.25
Cu	26.90	78.60	55.62					
Pb	7.80	19.60	14.28		K_2O/Na_2O	0.16	0.54	0.40
Zn	36.00	59.00	53.00		Mg #	54.40	59.26	56.87
W	0.50	0.70	0.60		A /CNK	0.79	0.94	0.84
Rb	6.60	35.80	20.52		Sr/Y	17.06	25.84	21.07
Ba	249.00	470.00	355.20		Nb/Ta	9.33	37.00	17.97
Sr	244.00	387.60	322.60		Y/Nb	3.67	6.52	4.82
Ta	0.10	0.30	0.22		Nb/La	0.11	0.39	0.24
Nb	2.50	3.90	3.30		Ce/Pb	1.24	6.49	2.63
Hf	1.30	2.20	1.84		Zr/Sm	18.45	26.22	23.06
Zr	57.40	106.20	78.38		(La/Lu)n	3.97	8.72	6.32
Y	14.30	16.30	15.30		(La/Sm)n	2.46	3.28	2.81
Th	2.70	3.00	2.84		(Gd/Lu)n	1.29	1.62	1.45
U	0.70	0.90	0.78		(La/Yb)n	3.81	8.81	6.09
Ga	13.50	15.80	14.16		(Eu/Eu*)n	0.77	0.84	0.81

Mg# (mg-number) = molar 100xMgO/(MgO+$Fe_2O_3^T$). LOI = loss on ignition, Eu* = $(Sm+Gd)_N/2$

In the SiO_2 versus (Na_2O+K_2O) diagram (Figure 3a), the majority of the samples plot on the gabbro area and a little gabroic diorite area (Figure 3a). All of the samples are subalkalen in characters and have low to medium-K content in the K_2O versus SiO_2 diagram (Figure 3b).

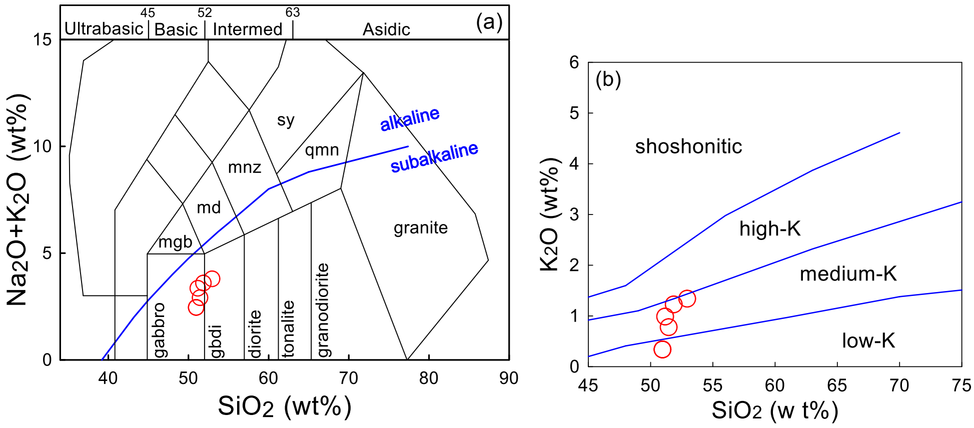

Figure 3. (a) (Na_2O+K_2O) versus SiO_2 diagram [51], (b) K_2O versus SiO_2 diagram [52] for the samples from the Büyükdüz Gabbro

Major and trace element exchange diagrams (Harker diagrams) are given in Figure 4 and 5. In the major elements versus SiO_2 diagrams, Fe_2O_3, MgO, CaO, P_2O_5 and TiO_2 decrease, and K_2O, Na_2O and Al_2O_3 increase with increasing SiO_2 values (Figure 4). In the trace element versus SiO_2 diagrams, Ni, Sr and Y show a negative corelation with the increasing SiO_2, while Ba, Rb, Zr, La, Pb and Nb show a positive correlation (Figure 5).

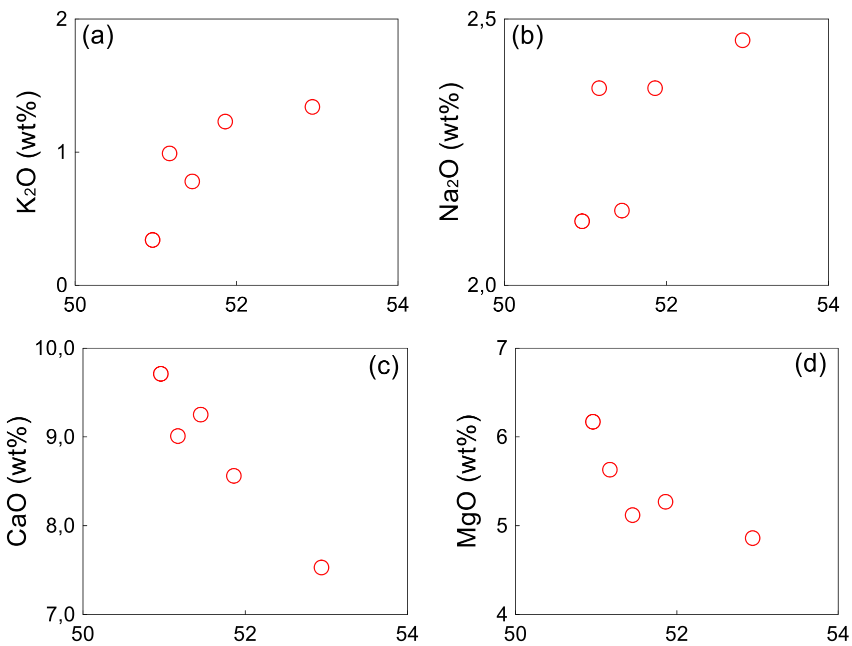

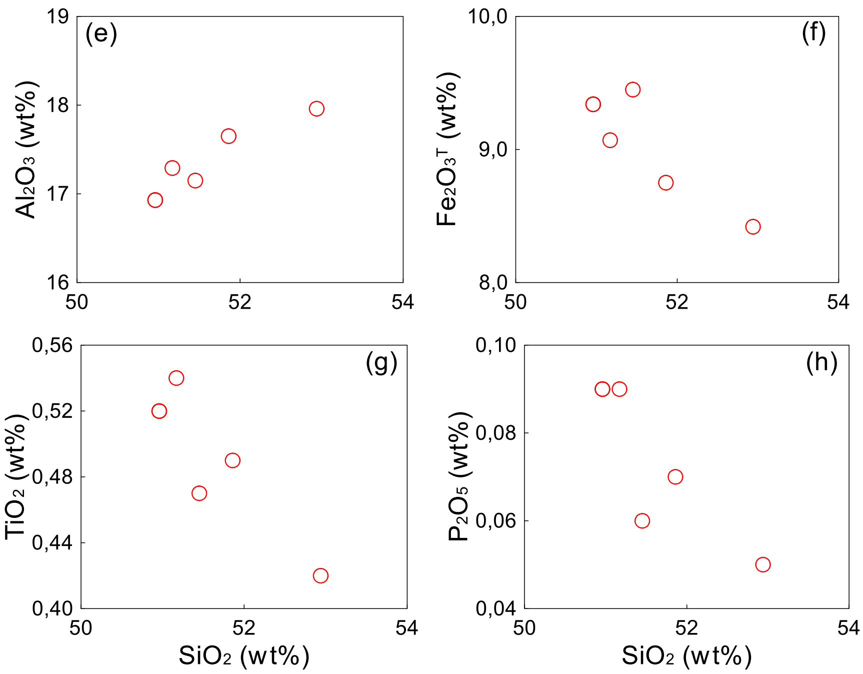

Figure 4. SiO_2 versus major element variation diagrams of the rocks from the Büyükdüz Gabbro

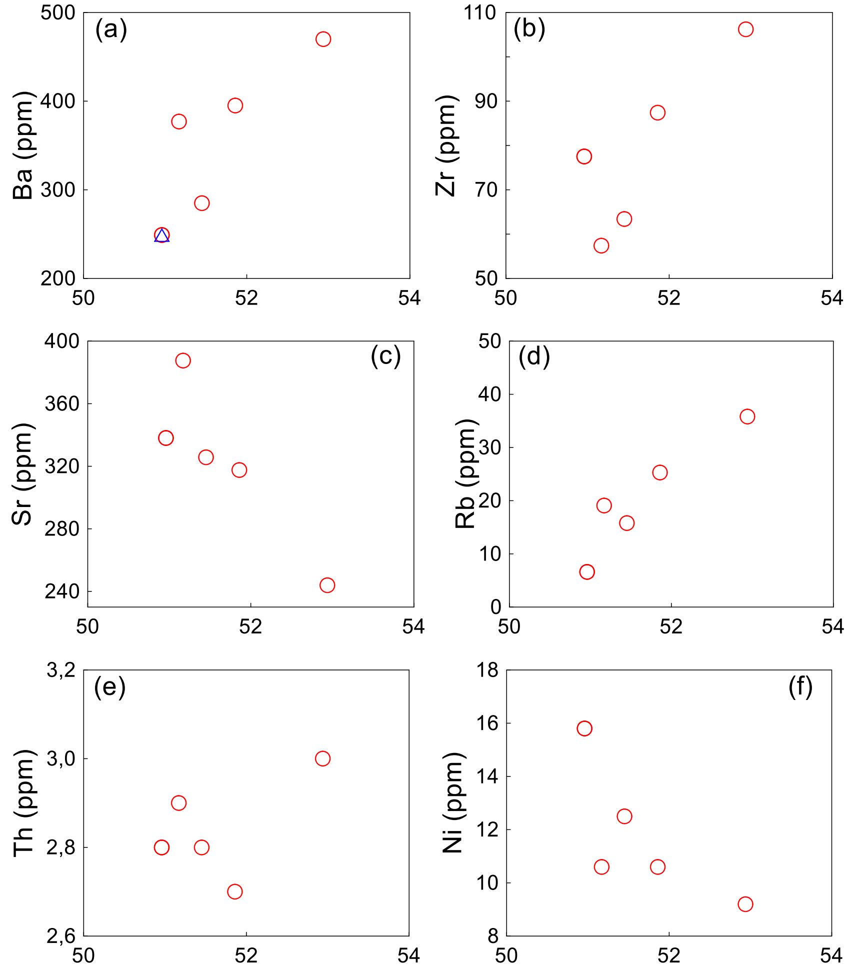

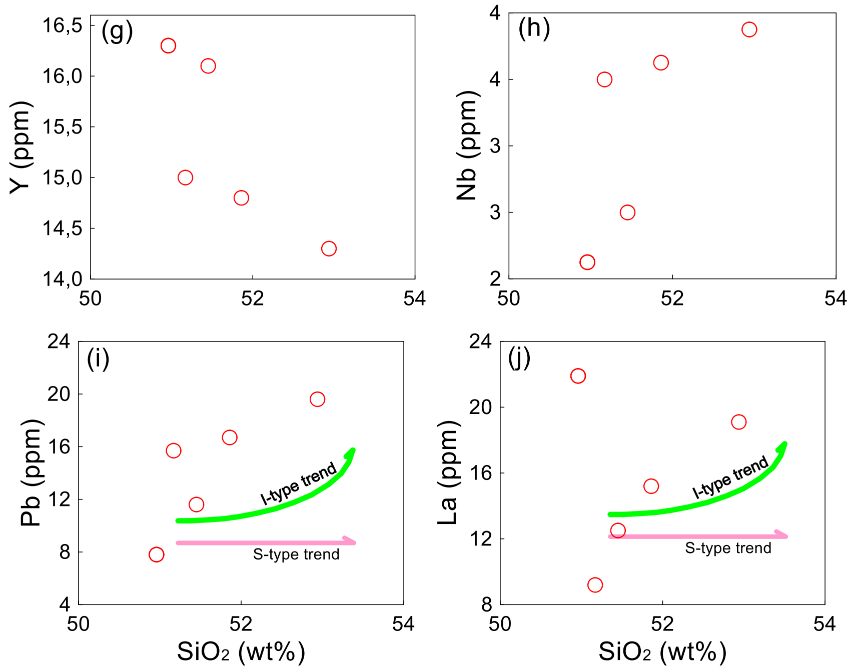

Figure 5. SiO_2 versus trace element variation diagrams of the rocks from the Büyükdüz Gabbro

In the trace element variation diagram normalized to the primitive mantle [53], the samples are chacterized by enrichment in LILEs and depletion in high-field strength elements (HFSEs) (Figure 6a). The negative Nb, Ta, P, Ti and positive Pb anomalies are seen in the samples (Figure 6a).

According to chondrite-normalized (normalization values [54]) rare earth element diagrams (Figure 6b), the studied samples show enrichment in LREEs with $(La/Sm)_N$ values of 2.46-3.28, and $(La/Yb)_N$ values of 3.81-8.81. The $(La/Lu)_N$ values of the samples are between 3.97 and 8.72, and $(Gd/Lu)_N$ values are between 1.29 and 1.62 (Figure 5b). Eu_n values of the samples are less than 1, and they show negative Eu_N (Eu/Eu*) anamolies of 0.77-0.84 (Figure 6b).

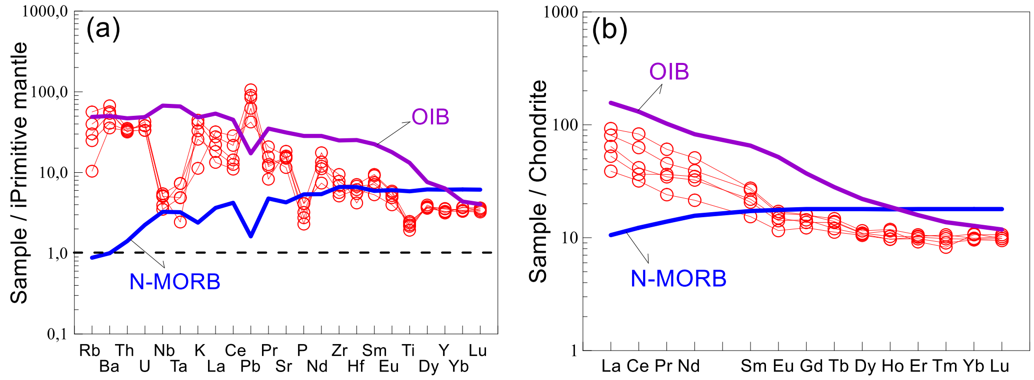

Figure 6. (a) Primitive mantle-normalized [53] trace element patterns, (b) Chondrite-normalized [54] rare earth element patterns for the rock samples from the Büyükdüz Gabbro

4.2.2. Tectonic setting

In the SiO_2 versus ASI (molar $Al_2O_3/(CaO+Na_2O+K_2O)$) diagram, the samples show metaluminous in characters and plot on the I-type field in the Nb versus 10000GA/Al diagram (Figure 7 a and b).

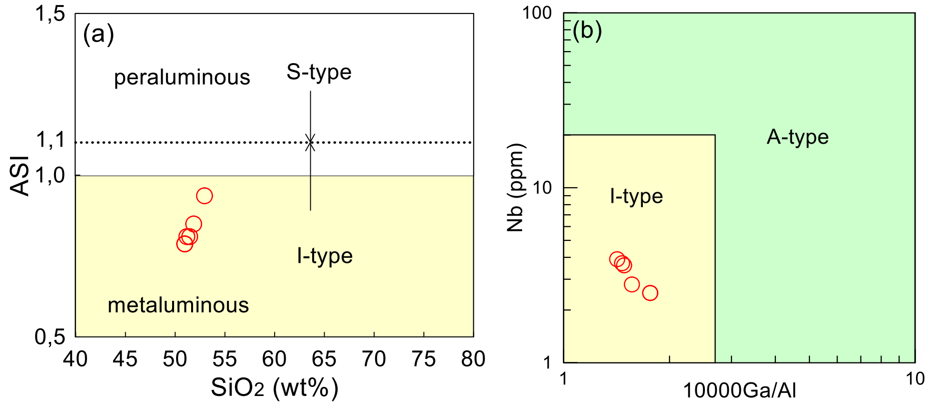

Figure 7. (a) SiO_2 versus ASI diagram (fields: [55,56], (b) Nb versus 10000Ga/La diagram [57] of the samples from the Büyükdüz Gabbro

The Sr/Y ratios of the studied samples are between 17.1 and 25.8, and plot on the volcanic arc field in the Sr/Y versus Y diagram (Figure 8a). In the Rb/Zr versus Y diagram (Figure 8b), the samples have in the normal arc maturity.

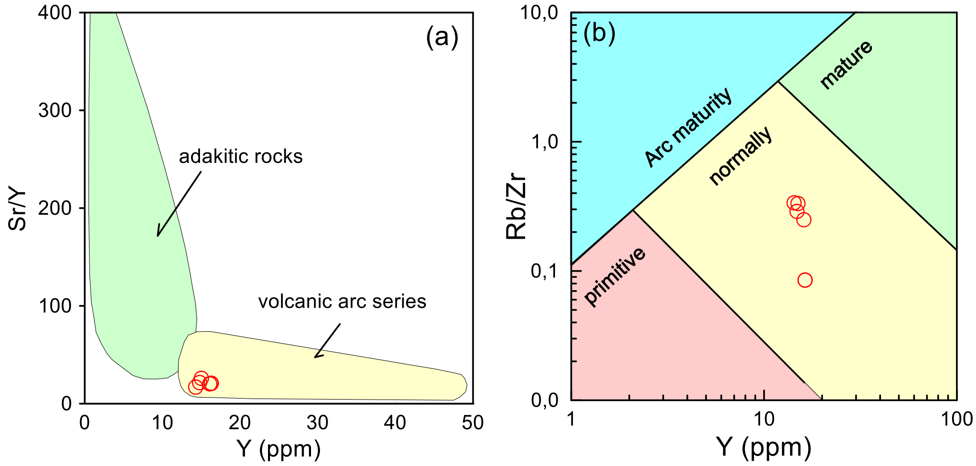

Figure 8. (a) Sr/Y versus Y diagram [58], (b) Y versus Rb/Zr diagram [59] of the samples from the Büyükdüz Gabbro

In the Rb versus (Yb+Ta) diagram [57], the samples fall in the volcanic arc granitoid (VAG) field (Figure 9a). Similarly, they are located in the VAG field in the Ta versus Yb, Nd versus Y and Ta/Yb versus Ta+Yb diagrams (Figure 9b-d).

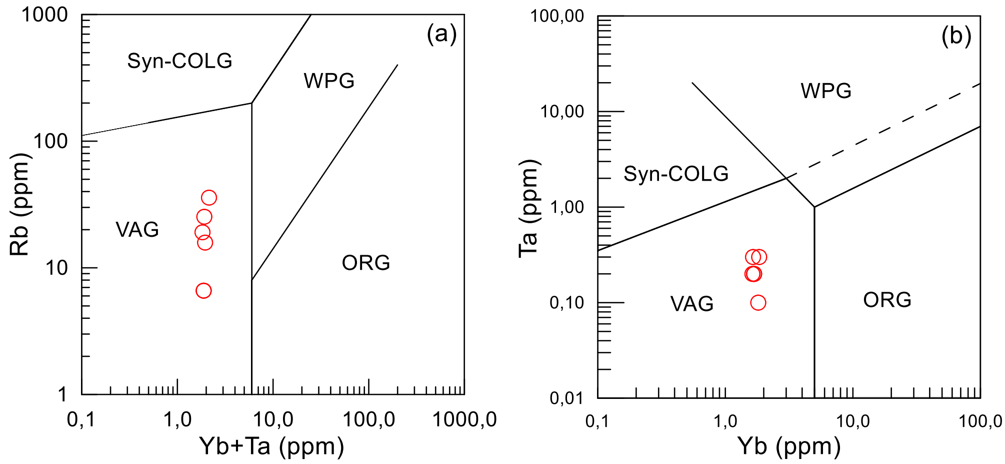

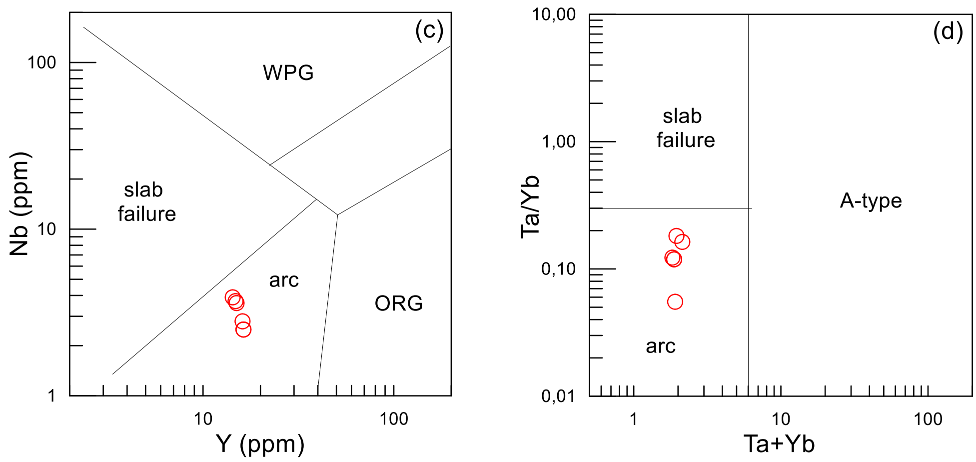

Figure 9. (a) Rb versus (Yb+Ta) diagram, (b) Ta versus Yb diagram [57], (c) Nb versus Y diagram, (d) Ta/Yb versus Ta+Yb diagram of the samples from the Büyükdüz Gabbro

5. Discussion and conclusions

Most of the whole-rock major and trace element variation trends with SiO_2 for the studied samples most likely reflect fractional crystallization. The decreases in MgO, Fe_2O_3, CaO, P_2O_5, TiO_2 and Sr with increasing SiO_2 point to a role for the fractionation of plagioclase, clinopyroxene, amphibole and Fe-Ti oxide (Figures 4 and 5).

The Ba/Sr ratios of the studied samples exhibits negative correlation with increasing Sr contents, which can be explained by plagioclase fractionation (Figure 10a). In the CaO versus Y plot [60], all samples has an J-type trend, suggesting clinopyroxene and hornblende fractionation (Figure 10b).

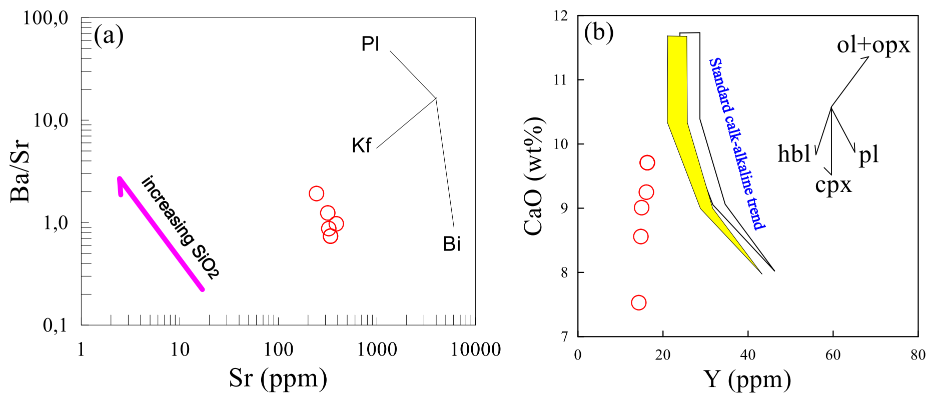

Figure 10. (a) Ba/Sr versus Sr diagram; (b) CaO versus Y diagram [60] from the studied rocks rocks.

The samples of the studied gabroic rocks are also characterized by negative Nb, Ta, Ti and P and positive Rb, K, Th, and Pb anomalies as well as enrichment in LILEs and LREEs (Figures 6 and 7). These features are commonly found in crustal rocks. Experimental data also show that the rocks formed by partial melts of the lower and middle crust should have Mg numbers (Mg#) less than 41 in the range of $SiO_2 \leq 51$-65 [61,62]. The studied samples have low SiO_2 content of 51-53 wt.% and high Mg# (53-56). If the source magma was derived directly from partial melting of mafic lower crust, then the primitive samples from the studied rocks should have low Mg# [61] in the range of $SiO_2 \leq 51$-65. However, such is not the case, and the Mg numbers of the studied mafic rocks are clearly higher than those from experimental crustal melts (<41), as shown in Figure 11a. For this reason, the studied samples may be derived from mantle lithologies, rather than from mafic-felsic crustal lithologies.

Some authors [63,64] suggested that, high Nb/La ratios (~ >1) demonstrate an OIB like asthenospheric mantle source for basaltic magmas, and lower ratios (~ <0.5) display a lithospheric mantle source. The Nb/La (0.1–0.4) ratios of the samples indicate a lithospheric mantle source (Table 1), as shown in Figure 11b. In the Nb/Th versus Nb diagram, all samples plot in the arc fields (Figure 11c). The Th/Yb versus Ta/Yb [65] (Figure 11d) diagram, the studied rock samples form a trend sub–parallel to the mantle array but shifted to higher Th/Yb ratios. This indicates melt derivation from a source, which had been previously enriched (or metasomatized) by fluids derived from an subduction processes.

All geochemical data has shown that the rocks of the Büyükdüz Gabbro represent a period of (immature) arc development and probably formed during an early stage of convergent plate boundary tectonics. The magmatism is related to subduction of the Neo-Tethyan Ocean beneath the Eurasian plate along the IAE suture zone during the Late Cretaceous.

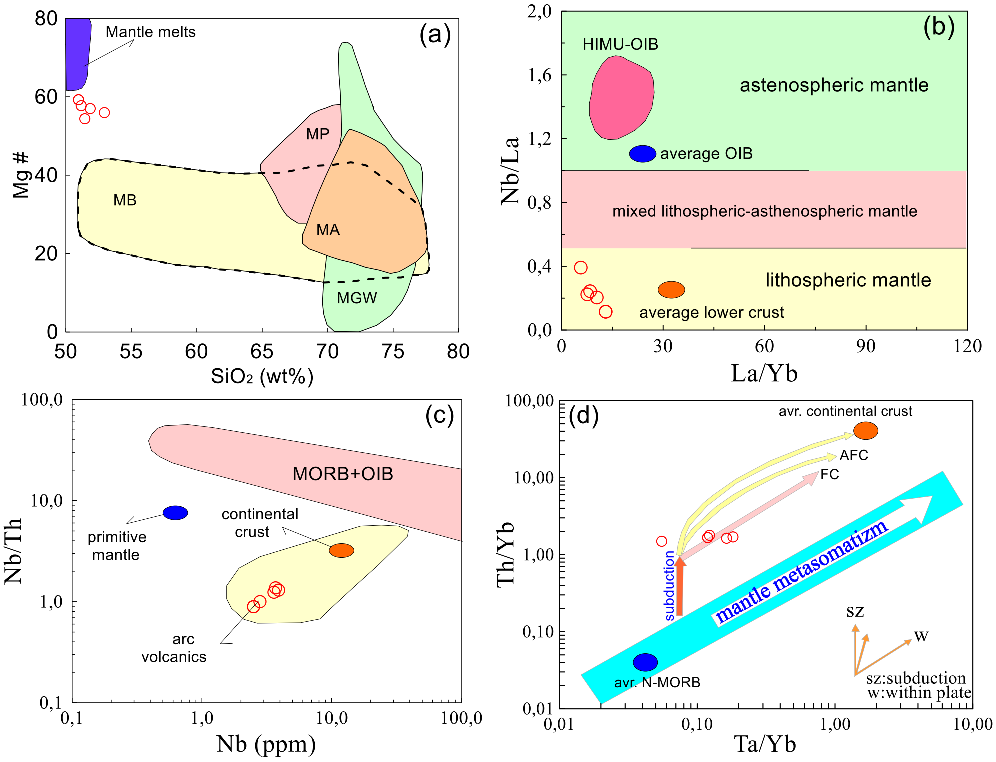

Figure 11. (a) Mg# versus SiO_2, (b) Nb/La versus La/Yb plots, (c) Nb/Th versus Nb, (d) Th/Yb versus Ta/Yb diagrams from the studied rocks. Compositions of continental crust, mid-ocean ridge basalts (MORB), ocean-island basalts (OIB) and arc volcanics after [66]; Average OIB is after [67] and average lower crust is after [68]. Dashed lines separating fields of the asthenospheric, lithospheric and mixed mantle are plotted based on data given in [64].

Acknowledgement
This study was partially supported by TÜBİTAK project (Project No: 109Y052).

References

[1] Şengör AMC, Yılmaz Y. Tethyan evolution of Turkey: a plate tectonic approach. Tectonophysics 1981; 75:181–241.
[2] Okay A, Şahintürk Ö. Geology of the eastern Pontides. In: Robinson AG (Ed.) Regional and petroleum geology of the Black Sea and surrounding region. Am Assoc Pet Geol Mem 1997; 68:291–311.
[3] Yücel C, Aydınçakır E, Kaygusuz A, Arslan M, Yi K, Jeong YJ, Cicerali D. Petrogenesis of Late Cretaceous A-type plutonic rocks from the Eastern Pontides Orogenic Belt (NE Turkey): constraints from zircon U-Pb geochronology, zircon Lu-Hf and whole-rock Sr-Nd-Pb-Hf isotopes. Int Geol Rev 2023; 00:1–24.
[4] Aydınçakır E, Yücel C, Kaygusuz A, Bilici Ö, Yi K, Jeong YJ, Gülöğlu ZS. Magmatic evolution of the Calc-alkaline Middle Jurassic igneous rocks in the eastern pontides, NE Turkey: insights from geochemistry, whole-rock Sr-Nd-Pb, in situ zircon Lu-Hf isotopes, and U-Pb geochronology. Int Geol Rev 2023; 00:1–22.
[5] Temizel İ, Arslan M, Abdioğlu Yazar E, Aslan Z, Kaygusuz A, Baki Eraydın T. Zircon U-Pb geochronology and petrology of the tholeiitic

gabbro from the Kovanlık (Giresun) area: Constraints for the Late Cretaceous bimodal arc magmatism in the Eastern Pontides Orogenic Belt, NE Turkey. Lithos 2022; 428–429.

[6] Aydınçakır E, Yücel C, Ruffet G, Gücer MA, Akaryalı E, Kaygusuz A. Petrogenesis of post-collisional Middle Eocene volcanism in the Eastern Pontides (NE, Turkey): Insights from geochemistry, whole-rock Sr-Nd-Pb isotopes, zircon U-Pb and 40Ar-39Ar geochronology. Geochemistry 2022:125871.

[7] Kaygusuz A, Arslan M, Temizel İ, Yücel C, Aydınçakır E. U–Pb zircon ages and petrogenesis of the Late Cretaceous I-type granitoids in arc setting, Eastern Pontides, NE Turkey. J African Earth Sci 2021; 174:104040.

[8] Vural A, Kaygusuz A. Geochronology, petrogenesis and tectonic importance of Eocene I-type magmatism in the Eastern Pontides, NE Turkey. Arab J Geosci 2021; 14.

[9] Arslan M, Temizel İ, Ackerman L, Yücel C, Abdioğlu Yazar E. Highly siderophile element and Os isotope systematics of the Cenozoic volcanic rocks from the Eastern Pontides, NE Turkey: Constraints on the origin and evolution of subcontinental mantle-derived magmas. Lithos 2022; 410–411.

[10] Kaygusuz A, Siebel W, Şen C, Satır M. Petrochemistry and petrology of I-type granitoids in an arc setting: The composite Torul pluton, Eastern Pontides, NE Turkey. Int J Earth Sci 2008; 97:739–764.

[11] Kaygusuz A, Arslan M, Siebel W, Sipahi F, Ilbeyli N, Temizel İ. LA-ICP MS zircon dating, whole-rock and Sr-Nd-Pb-O isotope geochemistry of the Camiboğazi pluton, Eastern Pontides, NE Turkey: Implications for lithospheric mantle and lower crustal sources in arc-related I-type magmatism. Lithos 2014; 192–195:271–290.

[12] Kaygusuz A, Vural A. Büyükdüz Gabrosunun (Camiboğazı/Trabzon) tüm-kayaç jeokimyasal özellikleri. 8th Internatıonal Zeugma Conference On Scientific Research, July 15-17, Gaziantep, Turkey. 2022:469–478.

[13] Özsayar T, Pelin S, Gedikoğlu A. Doğu Pontidlerde Kretase. KTÜ Yer Bilim Derg 1981; 1:65–114.

[14] Topuz G, Altherr R, Kalt A, Satir M, Werner O, Schwarz WH. Aluminous granulites from the Pulur complex, NE Turkey: A case of partial melting, efficient melt extraction and crystallisation. Lithos 2004; 72:183–207.

[15] Topuz G, Altherr R, Siebel W, Schwarz WH, Zack T, Hasözbek A, Barth M, Satir M, Şen C. Carboniferous high-potassium I-type granitoid magmatism in the Eastern Pontides: The Gümüşhane pluton (NE Turkey). Lithos 2010; 116:92–110.

[16] Dokuz A. A slab detachment and delamination model for the generation of Carboniferous high-potassium I-type magmatism in the Eastern Pontides, NE Turkey: The Köse composite pluton. Gondwana Res 2011; 19:926–944.

[17] Kaygusuz A, Aydınçakır E, Yücel C, Atay HE. Petrographic and geochemical characteristics of Carboniferous plutonic rocks around Erenkaya (Gümüşhane, NE Turkey). J Eng Res Appl Sci 2021; 10:1774–1778.

[18] Vural A, Kaygusuz A. Petrology of the Paleozoic plutons in Eastern pontides: Artabel Pluton (Gümüşhane, NE Turkey). J Eng Res Appl Sci 2019; 8:1216–1228.

[19] Kaygusuz A. Geochronological age relationships of Carboniferous Plutons in the Eastern Pontides (NE Turkey). J Eng Res Appl Sci 2020; 9:1299–1307.

[20] Karslı O, Dokuz A, Kandemir R. Subduction-related Late Carboniferous to Early Permian Magmatism in the Eastern Pontides, the Camlik and Casurluk plutons: Insights from geochemistry, whole-rock Sr–Nd and in situ zircon Lu–Hf isotopes, and U–Pb geochronology. Lithos 2016; 266–267:98–114.

[21] Kaygusuz A, Arslan M, Siebel W, Sipahi F, Ilbeyli N. Geochronological evidence and tectonic significance of Carboniferous magmatism in the southwest Trabzon area, eastern Pontides, Turkey. Int Geol Rev 2012; 54:1776–1800.

[22] Kaygusuz A, Arslan M, Sipahi F, Temizel İ. U–Pb zircon chronology and petrogenesis of Carboniferous plutons in the northern part of the Eastern Pontides, NE Turkey: Constraints for Paleozoic magmatism and geodynamic evolution. Gondwana Res 2016; 39:327–346.

[23] Saydam Eker Ç. Petrography and geochemistry of Eocene sandstones from eastern Pontides (NE TURKEY): Implications for source area weathering, provenance and tectonic setting. Geochemistry Int 2012; 50:683–701.

[24] Ağar Ü. Demirözü (Bayburt) ve Köse (Kelkit) bölgesinin jeolojisi. İstanbul Üniversitesi, 1977.

[25] Dokuz A, Karslı O, Chen B, Uysal I. Sources and petrogenesis of Jurassic granitoids in the

Yusufeli area, Northeastern Turkey: Implications for pre- and post-collisional lithospheric thinning of the eastern Pontides. Tectonophysics 2010; 480:259–279.

[26] Ustaömer T, Robertson AHF, Ustaömer PA, Gerdes A, Peytcheva I. Constraints on Variscan and Cimmerian magmatism and metamorphism in the Pontides (Yusufeli-Artvin area), NE Turkey from U-Pb dating and granite geochemistry. Geol Soc Spec Publ 2013; 372:49–74.

[27] Eyuboğlu Y, Dudas FO, Santosh M, Zhu DC, Yi K, Chatterjee N, Jeong YJ, Akaryalı E, Liu Z. Cenozoic forearc gabbros from the northern zone of the Eastern Pontides Orogenic Belt, NE Turkey: Implications for slab window magmatism and convergent margin tectonics. Gondwana Res 2016; 33:160–189.

[28] Karslı O, Dokuz A, Kandemir R. Zircon Lu-Hf isotope systematics and U–Pb geochronology, whole-rock Sr-Nd isotopes and geochemistry of the early Jurassic Gokcedere pluton, Sakarya Zone-NE Turkey: a magmatic response to roll-back of the Paleo-Tethyan oceanic lithosphere. Contrib to Mineral Petrol 2017; 172:31.

[29] Pelin S. Alucra (Giresun) güneydoğu yöresinin petrol olanakları bakımından jeolojik incelenmesi. Karadeniz Tek Üniversitesi Yayınları 1977:87–103.

[30] Aydınçakır E. Subduction-related Late Cretaceous high-K volcanism in the Central Pontides orogenic belt: constraints on geodynamic implications. Geodin Acta 2016; 28:379–411.

[31] Sipahi F, Akpınar İ, Saydam Eker Ç, Kaygusuz A, Vural A, Yılmaz M. Formation of the Eğrikar (Gümüşhane) Fe–Cu skarn type mineralization in NE Turkey: U–Pb zircon age, lithogeochemistry, mineral chemistry, fluid inclusion, and O-H-C-S isotopic compositions. J Geochemical Explor 2017; 182:32–52.

[32] Temizel İ, Arslan M, Yücel C, Abdioğlu Yazar E, Kaygusuz A, Aslan Z. U-Pb geochronology, bulk-rock geochemistry and petrology of Late Cretaceous syenitic plutons in the Gölköy (Ordu) area (NE Turkey): Implications for magma generation in a continental arc extension triggered by slab roll-back. J Asian Earth Sci 2019; 171:305–320.

[33] Aydın F, Oğuz Saka S, Şen C, Dokuz A, Aiglsperger T, Uysal İ, Kandemir R, Karslı O, Sarı B, Başer R. Temporal, geochemical and geodynamic evolution of the Late Cretaceous subduction zone volcanism in the eastern Sakarya Zone, NE Turkey: Implications for mantle-crust interaction in an arc setting. J Asian Earth Sci 2020; 192:104217.

[34] Vural A, Kaygusuz A, Akpınar İ. Petrological characteristics of Late Cretaceous volcanic rocks of Demirören (Gümüşhane, NE Turkey) region. J Eng Res Appl Sci 2021; 10:1828–1842.

[35] Vural A, Kaygusuz A. Petrographic and geochemical characteristics of Late Cretaceous volcanic rocks in the vicinity of Avliyana (Gümüşhane, NE Turkey). J Eng Res Appl Sci 2021; 10:1796–1810.

[36] Köprübaşı N, Şen C, Kaygusuz A. Doğu Pontid adayayı granitoyidlerinin karşılaştırılmalı petrografik ve kimyasal özellikleri, KD Türkiye. Uygulamalı Yerbilim Derg 2000; 1:111–120.

[37] Kaygusuz A, Saydam Eker Ç. Geochemical features and petrogenesis of Late Cretaceous subduction-related volcanic rocks in the Değirmentaşı (Torul/Gümüşhane) area, Eastern Pontides (NE Turkey). J Eng Res Appl Sci 2021; 10:1689–1702.

[38] Topuz G, Okay AI, Altherr R, Schwarz WH, Siebel W, Zack T, Satir M, Sen C. Post-collisional adakite-like magmatism in the Agvanis Massif and implications for the evolution of the Eocene magmatism in the Eastern Pontides (NE Turkey). Lithos 2011; 125:131–150.

[39] Arslan M, Temizel İ, Abdioğlu E, Kolaylı H, Yücel C, Boztuğ D, Şen C. 40Ar–39Ar dating, whole-rock and Sr–Nd–Pb isotope geochemistry of post-collisional Eocene volcanic rocks in the southern part of the Eastern Pontides (NE Turkey): implications for magma evolution in extension-induced origin. Contrib to Mineral Petrol 2013; 166:113–142.

[40] Aslan Z, Arslan M, Temizel İ, Kaygusuz A. K-Ar dating, whole-rock and Sr-Nd isotope geochemistry of calc-alkaline volcanic rocks around the Gümüşhane area: Implications for post-collisional volcanism in the Eastern Pontides, Northeast Turkey. Mineral Petrol 2014; 108:245–267.

[41] Eyuboğlu Y, Dudas FO, Thorkelson D, Zhu DC, Liu Z, Chatterjee N, Yi K, Santosh M. Eocene granitoids of northern Turkey: Polybaric magmatism in an evolving arc–slab window system. Gondwana Res 2017; 50:311–345.

[42] Temizel İ, Abdioğlu Yazar E, Arslan M, Kaygusuz A, Aslan Z. Mineral chemistry,

whole-rock geochemistry and petrology of Eocene I-type shoshonitic plutons in the Gölköy area (Ordu, NE Turkey). Bull Miner Res Explor 2018; 157:121–152.
[43] Kaygusuz A, Merdan Tutar Z, Yücel C. Mineral chemistry, crystallization conditions and petrography of Cenozoic volcanic rocks in the Bahçecik (Torul/Gumushane) area, Eastern Pontides (NE Turkey). J Eng Res Appl Sci 2017; 6:641–651.
[44] Kaygusuz A, Gucer MA, Yücel C, Aydınçakır E, Sipahi F. Petrography and crystallization conditions of Middle Eocene volcanic rocks in the Aydıntepe-Yazyurdu (Bayburt) area, Eastern Pontides (NE Turkey). J Eng Res Appl Sci 2019; 8:1205–1215.
[45] Cicerali D, Arslan M, Abdioğlu Yazar E, Yücel C, Temizel İ, Park S, Schroeder PA. Mineralogy, chemistry, and genesis of zeolitization in Eocene tuffs from the Bayburt area (NE Turkey): Constraints on alteration processes of acidic pyroclastic deposits. J African Earth Sci 2020; 162.
[46] Yücel C, Arslan M, Temizel İ, Abdioğlu Yazar E, Ruffet G. Evolution of K-rich magmas derived from a net veined lithospheric mantle in an ongoing extensional setting: Geochronology and geochemistry of Eocene and Miocene volcanic rocks from Eastern Pontides (Turkey). Gondwana Res 2017; 45:65–86.
[47] Kaygusuz A, Yücel C, Arslan M, Sipahi F, Temizel İ, Çakmak G, Güloglu ZS. Petrography, mineral chemistry and crystallization conditions of Cenozoic plutonic rocks located to the north of Bayburt (Eastern Pontides, Turkey). Bull Miner Res Explor 2018; 157:75–102.
[48] Kaygusuz A, Yücel C, Aydınçakır E, Gücer MA, Ruffet G. 40Ar–39Ar dating, whole-rock and Sr-Nd isotope geochemistry of the Middle Eocene calc-alkaline volcanic rocks in the Bayburt area, Eastern Pontides (NE Turkey): Implications for magma evolution in an extension-related setting. Mineral Petrol 2022; 116:379–399.
[49] Kaygusuz A, Yücel C, Arslan M, Temizel İ, Yi K, Jeong YJ, Siebel W, Sipahi F. Eocene I-type magmatism in the Eastern Pontides, NE Turkey: insights into magma genesis and magma-tectonic evolution from whole-rock geochemistry, geochronology and isotope systematics. Int Geol Rev 2020; 62:1406–1432.
[50] Streckeisen A. To each plutonic rock its proper name. Earth Sci Rev 1976; 12:1–33.
[51] Middlemost EAK. Naming materials in the magma/igneous rock system. Earth Sci Rev 1994; 37:215–224.
[52] Le Maitre RW, Bateman P, Dudek A, Keller J, Lameyre J, Le Bas MJ, Sabine PA, Schmid R, Sorensen H, Streckeisen A, Wooley AR, Zanettin B. A classification of igneous rocks and glossary of terms. Blackwell, Oxford 1989:193 pp.
[53] Sun SS, McDonough WF. Chemical and isotopic systematics of oceanic basalts: implications for mantle composition and processes. Geol Soc London, Spec Publ 1989; 42:313–345.
[54] Taylor SR, McLennan SM. The Continental Crust; Its Composition and Evolution. Geosci Text, Blackwell Sci Publ 1985.
[55] Chappell BW, White AJR. Two contrasting granite types. Pacific Geol 1974; 8:173–174.
[56] Shand SJ. Eruptive rocks. Their genesis, composition, classification and their relation to ore-deposits. 3rd Ed J Wiley Sons, New York 1947:488 pp.
[57] Pearce JA, Harris NBW, Tindle AG. Trace element discrimination diagram for the tectonic interpretation of granitic rocks. J Petrol 1984; 25:956–983.
[58] Defant MJ, Drummond MS. Derivation of some modern arc magmas by melting of young subducted lithosphere. Nature 1990; 347:662–665.
[59] Brown G, Thorpe R, Webb P. The geochemical characteristics of granitoides in contrasting arcs and comments on magma source. J Geol Soc London 1984; 141:413–426.
[60] Lambert RJ, Holland JG. Yttrium geochemistry applied to petrogenesis utilizing calcium-yttrium relationships in minerals and rocks. Geochim Cosmochim Acta 1974; 38:1393–1414.
[61] Rapp RP, Watson EB. Dehydration melting of metabasalt at 8–32 kbar: Implications for continental growth and crust–mantle recyling. J Pet 1995; 36:891–931.
[62] Sisson TW, Ratajeski K, Hankins WB, Glazner AF. Voluminous granitic magmas from common basaltic sources. Contrib Miner Pet 2005; 148:635–661.
[63] Bradshaw TK, Smith EI. Polygenetic Quaternary volcanism at Crater Flat, Nevada. J Volcanol Geoth Res 1994; 63:165–182.
[64] Smith EI, Sanchez A, Walker JD, Wang K. Geochemistry of mafic magmas in the

Hurricane Volcanic field, Utah: implications for small- and large-scale chemical variability of the lithospheric mantle. J Geol 1999; 107:433–448.

[65] Pearce JA, Bender JF, De Long SE, Kidd WSF, Low PJ, Güner Y, Şaroğlu F, Yılmaz Y, Moorbath S, Mitchell JJ. Genesis of collision volcanism in eastern Anatolia Turkey. J Volcanol Geoth Res 1990; 44:189–229.

[66] Schmidberger SS, Hegner E. Geochemistry and isotope ststematics of calc-alkaline volcanic rocks from the Saar-Nahe basin (SW Germany)-implications for Late Variscan orogenic development. Contrib to Mineral Petrol 1999; 135:373–385.

[67] Fitton JG, James D, Leeman WP. Basic magmatism associated with Late Cenozoic extension in the western United States: compositional variations in space and time. J Geophys Res 1991; 96:13693–13712.

[68] Chen W, Arculus RJ. Geochemical and isotopic characteristics of lower crustal xenoliths, San Francisco Volcanic Field, Arizona, U.S.A. Lithos 1995; 36:203–225.